Available online at www.sciencedirect.com
ScienceDirect
Aquacultural Engineering 35 (2006) 292–299
aquacultural engineering
www.elsevier.com/locate/aqua-online

Drag force acting on biofouled net panels

M. Robinson Swift [a,*], David W. Fredriksson [b], Alexander Unrein [a], Brett Fullerton [c], Oystein Patursson [c,d], Kenneth Baldwin [c]

[a] *Mechanical Engineering Department, Kingsbury Hall, University of New Hampshire, Durham, NH 03824, USA*
[b] *Department of Naval Architecture and Ocean Engineering, United States Naval Academy, Annapolis, MD 21402, USA*
[c] *Jere A. Chase Ocean Engineering Center, University of New Hampshire, Durham, NH 03824, USA*
[d] *Faculty of Science and Technology, University of the Faroe Islands, FO-100 Torshavn, Faroe Islands*

Received 8 September 2005; accepted 21 March 2006

Abstract

Measurements were made to assess the increase in drag on aquaculture cage netting due to biofouling. Drag force was obtained by towing net panels, perpendicular to the incident flow, in experiments conducted in a tow tank and in the field. The net panels were fabricated from netting stretched within a 1 m^2 pipe frame. They were towed at various speeds, and drag force was measured using a bridle-pulley arrangement terminating in a load cell. The frame without netting was also drag tested so that net-only results could be obtained by subtracting out the frame contribution. Measurements of drag force and velocity were processed to yield drag coefficients.

Clean nets were drag tested in the University of New Hampshire (UNH) 36.5 m long tow tank. Nets were then exposed to biofouling during the summer of 2004 at the UNH open ocean aquaculture demonstration site 1.6 km south of the Isles of Shoals, New Hampshire, U.S.A. Nine net panels were recovered on 6 October 2004 and immediately drag tested at sea to minimize disturbing the fouling communities. The majority of the growth was skeleton shrimp (*Caprella* sp.) with some colonial hydroids (*Tubularia* sp.), blue mussels (*Mytilus edulus*) and rock borer clams (*Hiatella actica*). Since the deployment depth was 15 m (commensurate with submerged cages at the site), no algae were present. The net panels had been subject to several different antifouling treatments, so the extent of growth varied amongst the panels. Drag force measurements were made using a bridle-pulley-load cell configuration similar to that employed in the tow tank. Fixtures and instruments were mounted on an unpowered catamaran that was towed alongside a workboat. Thus, the catamaran served as the ''carriage'' for field measurements.

Increases in net-only drag coefficient varied from 6 to 240% of the clean net values. The maximum biofouled net drag coefficient was 0.599 based on net outline area. Biofouled drag coefficients generally increased with solidity (projected area of blockage divided by outline area) and volume of growth. There was, however, considerable scatter attributed in part to different mixes of species present.

Keywords: Drag force; Drag coefficient; Biofouling; Nets; Net-pens; Net panels; Cages; Tow tank

1. Introduction

The purpose of this study was to measure the increase in fluid drag on fish cage netting due to naturally occurring biofouling. Because the drag force acting on fish cage netting constitutes a major mechanism by which wave and current loads are imparted to net pens (Palczynski, 2000; Fredriksson et al., 2003), quantifying this mechanism is important to the design of open ocean aquaculture net pen systems. Recent field experience gained with two cages deployed one nautical mile south of White Island, Isles of Shoals,

* Corresponding author. Tel.: +1 603 862 1837; fax: +1 603 862 1865.
E-mail address: mrswift@cisunix.unh.edu (M.R. Swift).

0144-8609/$ – see front matter © 2006 Elsevier B.V. All rights reserved.
doi:10.1016/j.aquaeng.2006.03.002

NH indicates that marine growth on cages is a serious problem and will certainly alter the drag characteristics of the netting significantly.

Previous work on clean net drag forces includes drag coefficient information reported by Aarsnes et al. (1990). They provide a formula for the drag coefficient as a function of solidity (actual net thread projected area normalized by the outline area) and angle of incidence. The formula is based on accumulated tow tank data, and the effects of marine growth were not considered. In computer modeling, net drag has been calculated by representing the net threads as cylinders and using a Morison equation approach (Tsukrov et al., 2000). More recent finite element developments include the use of ''consistent net elements'' which depend on an understanding of fluid dynamic drag on net panels larger than mesh size but smaller than overall cage dimensions (Tsukrov et al., 2003). Lader et al. (2001) and Lader and Fredheim (2003), on the other hand, use a ''super-element'' formulation in which hydrodynamics forces are computed using lift and drag coefficients applied to four-sided net sections.

To improve our understanding of net drag in general and to characterize the effects of biofouling, framed net panels were tow tested at normal incidence to measure drag force as a function of speed. Experiments using ''clean'' netting were done under laboratory conditions in a tow tank, while biofouled net panel tests were carried out in the field. Tow tank measurements were used for the clean nets because the incident water environment was quiet, the tow platform rested on a fixed track, the instrumentation was protected, and the test schedule was not subject to weather or daylight limitations. The biofouled measurements, on the other hand, had to be done in seawater in order to minimize disturbance of the growth. A direct comparison of procedures (Unrein, 2004) indicated that results would be the same under field conditions of low ambient turbulence and sea state, as well as constant vessel tow speed. Experimental procedures were worked out in preliminary studies (Fullerton et al., 2002, 2003; Kurgan, 2003), which indicated that marine growth can increase net drag substantially.

The approach used in this study was to measure drag of clean panels in the University of New Hampshire (UNH) tow tank, deploy the panels at the Open Ocean Aquaculture (OOA) site at the Isles of Shoals, and re-measure drag force as a function of current speed after recovery. The study made use of nine 1 m × 1 m panels that were towed at normal incidence. Net panels were treated with antifouling agents of varying levels of toxicity; thus encouraging a range of growth on the recovered panels. Tow tank testing took place during April 2002 in UNH's 36 m long basin. Net panels were mounted below the tow carriage and pulled through the water at various speeds. A 112 lb capacity load cell attached through a bridle configuration was used to record the drag force acting on the panels. Tow speed was controlled by specifying the frequency of the electric motor operating the carriage. To confirm tow speed, which may vary slightly due to the tow load, two sets of optical light gates were used. Data was then analyzed using Microsoft Excel and MathCAD to obtain drag coefficients.

The net panels were exposed to marine growth at the OOA site for a 5-month period during the summer of 2004. The nine net panels were attached to a horizontal grid line making up the site's submerged, four-cage grid system. In a parallel study done at the same time, UNH marine biologists using similar (but smaller) net panels were monitoring and quantifying growth of biological communities. Immediately after recovery, the extent of biofouling was recorded by weighing and by photography, and drag measurements were completed. Tests took place in the nearby, relatively sheltered waters of Gosport Harbor, Isles of Shoals. The same approach as that used in tank testing was used with the exception that tows were performed in saltwater due to the sensitivity of the marine growth. The ''tow carriage'' used in the field was a catamaran configured platform towed alongside a small research vessel.

2. Theory

Fluid mechanics considerations are reviewed in order to define and provide context for measured quantities. Drag force is taken as the fluid dynamic force component acting on the object in the direction of the incident fluid velocity relative to the object (see, for example, White, 1999 or Berteaux, 1991). Drag is produced as a result of skin friction and pressure distribution (form drag). A functional form of drag, D, can be written as

$$D = f(d, V, \rho, \mu) \tag{1}$$

where d = length scale, V = fluid speed, ρ is fluid density and μ is the fluid dynamic viscosity.

From the Buckingham–Pi theorem, two dimensionless groups are functions of each other and can be expressed in the form:

$$\frac{D}{1/2\rho A_N V^2} = C_D(Re) \tag{2}$$

for a given body. In the above equation, A_N is the normal projected area, while C_D is the drag coefficient and is a function of Reynolds number:

$$Re = \frac{\rho V d}{\mu} \tag{3}$$

Eq. (2) serves as the basic defining equation for drag coefficient values obtained from the measurements. For low solidities, the net mesh is often thought of as a grid composed of perpendicular cylinders (ignoring intersection interactions). Taking this point of view, the drag coefficient of a clean net panel should bear some resemblance to that of a single cylinder for which roughness may play a role. For biofouled panels, the additional flow blockage and an increase in ''roughness'' and surface area are expected to increase drag.

3. Experimental procedures

3.1. Tank testing

Drag force measurement took place in UNH's 36.5 m long × 3.66 m wide × 2.44 m deep tow/wave tank using the tow carriage set-up shown in Fig. 1. Net panels consisted of treated and untreated, 1 m^2 netting tightly stretched within pipe frames, with each panel assigned a code number for identification purposes. As mounted from the carriage, each net panel was fully submerged, and no surface wave was generated during testing. The two vertical rods from the carriage to the net panel were free to rotate at each end, so they acted as two-force members imparting little horizontal force to the test panel. Thus the bridle, made of small diameter fish line attached to each of the four net panel corners, sustained the drag force. The bridle lead was run through the pulley shown and up to the load cell used to record the drag force magnitude. The general strategy was to measure the drag force of the entire net panel (net plus frame); then measure drag of just the pipe frame (without netting). The difference would then be the net (only) drag force.

Net panel frames were built for the experiment using 2.54 cm (1 in.) PVC pipe and elbows. Ballast was placed into the lower horizontal member so that the weight force slightly exceeded the buoyancy force and the panels were hydrostatically stable in an upright position. The inside dimension of the square frame (net size) was 1 m, a convenient size for handling and later scaling purposes. Net thread diameter was 1.59 mm, and the square mesh edge length was 2.54 cm. The net thread was braided Spectra, and the intersections were knotless. The solidity of the netting, defined as projected area of the threads divided by outline area, was 12.1%. The decision to use 1 m^2 netting was based in part on tow tank measurements by Kurgan (2003) using clean net with a slightly higher solidity. These showed negligible difference in net-only drag coefficient between 1 m and one quarter m square panels. Thus, the 1 m size was more than sufficient to minimize edge effects.

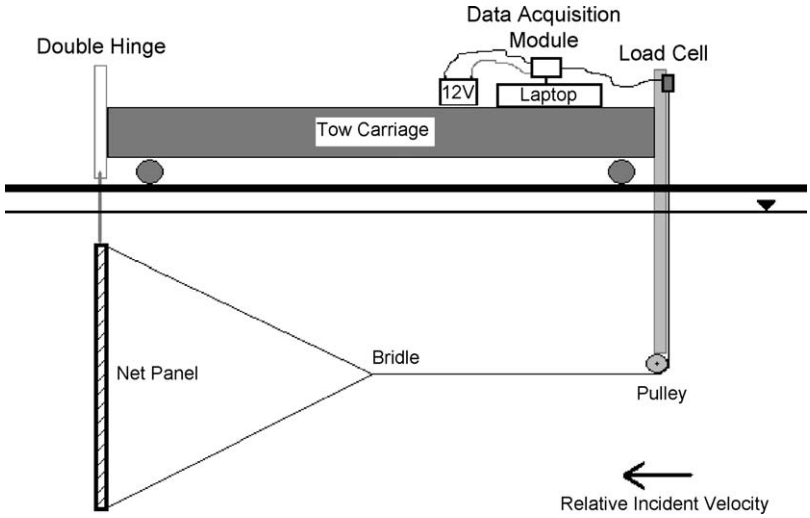

Fig. 1. Tow carriage set-up. The tow post is a 3.2 cm × 3.2 cm channel section with the open face aft, and it is 1.9 m forward of the net panel. The two vertical rods, pinned at each end, are 1.0 cm in diameter and hold the top of the net panel 29.8 cm below the free surface.

The tow carriage speed was governed by the electric motor frequency control. To confirm carriage velocity, two sets of optical light gates were also used. These light gates recorded the time for the carriage to travel a set distance of 1 m. An Interface 112 lb capacity SMT series load cell (model SMT2-112) was used to measure the drag force for these experiments. The load cell was calibrated several times using various lead weights of known value. Data was recorded at 1000 Hz using a laptop computer on the tow carriage. Raw data was saved for later processing using Microsoft Excel.

3.2. Exposure to biofouling

Before deployment, each net panel was weighed to determine net panel mass without biofouling. On 21 April 2004, the nine net panels were transported to the OOA site and secured to the mooring grid by divers. The attachment points were at a depth of 15 m and spread along a main horizontal crossing line near the center of the four-cage grid where they would be undisturbed. The intent was for the netting to accumulate the same type of fouling communities that would occur on new or newly cleaned netting covering submerged cages in the western North Atlantic. The exposure period included the summer months for which the majority of biofouling growth takes place (Greene, 2004). On 6 October 2004, the nine net panels were recovered by divers and transported 2 km north to Gosport Harbor, Isles of Shoals. A sheltered area with minimal wave activity, tidal current, wind and boat traffic was located for tow testing.

3.3. Field testing of biofouled panels

Before tow testing, each panel was weighed both out-of-water and in-water using spring scales. The panels were also photographed in their entirety and in close-ups using both front and back lighting. The backlit shots created large contrast between the light background and the dark netting/biofouling. This contrast was utilized later in processing the images to yield solidity.

The data acquisition system for testing biofouled panels in the field experiments replicated the tank testing set-up as much as possible. The equivalent tow carriage was an unpowered catamaran towed alongside and parallel to the research jet boat *Blue Fin* (see Figs. 2 and 3). When locked in the down position during test runs, the net panel-bridle-load cell arrangement was essentially the same as that shown for the tow carriage in Fig. 1. The catamaran-mounted fixture, however,

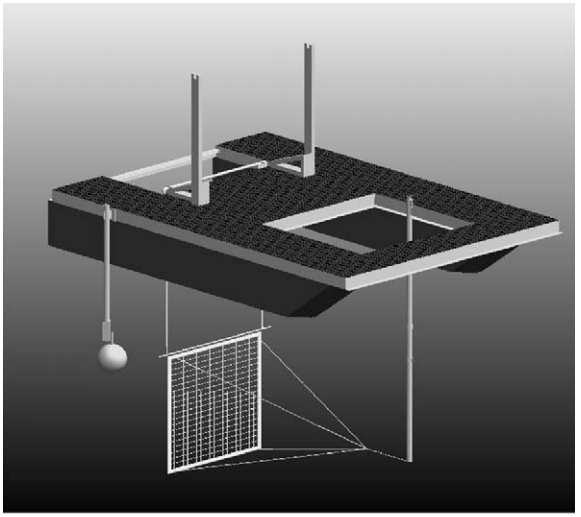

Fig. 2. The testing apparatus with the net panel in: (a) the lowered (testing) position and (b) the raised (mounting) position. The tow post is 2.33 m forward of the net panel, and the top of the net panel is 1.0 m below the surface.

Fig. 3. The data acquisition catamaran alongside the workboat *Blue Fin*.

included a folding frame arrangement allowing attachment and removal of panels from above deck level (Unrein, 2004). An InterOcean Systems S4 electromagnetic current meter was mounted to the starboard side to measure the platform velocity. A storage battery-inverter system was used to power two laptop computers onboard the *Blue Fin*, which were used to record data from the load cell and current meter. A comparison of field measurements of drag force on a clean panel with tow tank measurements of the same panel indicated that the catamaran-mounted system was equivalent to the tow tank system.

3.4. Data processing

Weight measurements for the clean and biofouled net panels, both in-air and in-water, were used to determine mass, density and volume of growth. The difference in corresponding weight between a biofouled and a clean panel yielded in-air and in-water weight of the growth mass. The difference between in-air and in-water weight of the growth provided the buoyancy force which, when divided by seawater density, yielded the growth volume.

On-site observations and later examination of photographs were employed to identify species present. The back-lighted photographs of representative sections of netting were processed to yield solidity. Using MatLab imaging capabilities, photographs were saved in 16 color gif format for which background colors (generally light bluish) were very different from those of biofouling and netting (dark). Color numbers corresponding to the background and those contributing to blockage were determined using a color chart. Then the color number for every pixel in the image was compared and the pixel assigned to either background or blockage. Solidity was then evaluated as number of biofouling plus netting pixels divided by total number of pixels.

In processing fluid velocity and force data sets, it was first necessary to identify sections that corresponded to steady state conditions. Velocity and force time series were plotted using a common time horizontal axis, and sections of unchanging velocity and force were isolated. Velocity and force were averaged over each section yielding one (velocity, force) pair. Force versus velocity data points were found for each of the nine panels and the empty frame. Next, a constant times V^2 curve was fit to each set of force versus velocity values by minimizing the mean square error. Subtracting the frame-only constant from each net panel constant yielded net-only results. The net-only constants were then used to compute drag coefficients according to Eq. (2).

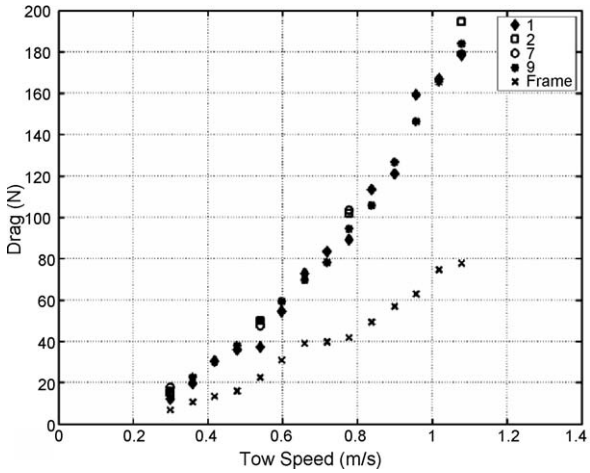

Fig. 4. Clean net drag force vs. velocity from tank testing.

4. Results

4.1. Clean panels

Though the netting and frame for all net panels were identical, three surface coating types were applied and one was left without treatment. One net panel from each of the four surface treatment categories was tank tested. Drag force as a function of velocity results are plotted for the four net panels tested, as well as an empty frame, in Fig. 4. Measurements were processed (see Section 3.4 Data processing) to yield clean, net-only drag coefficients which are given in Table 1. Two sets are listed—one based on area A taken as the outline area (1 m^2) and the other based on area A taken as the actual thread projected area (0.121 m^2).

4.2. Biofouled panels

The most ubiquitous growth was skeleton shrimp (*Caprella* sp.), which tended to fill the weave of netting contributing to solidity in all net panels. For the most

Table 1
Clean net drag coefficients from tank testing

Panel	Panels with similar coating	"Clean" C_D (based on $A_{outline}$)	"Clean" C_D (based on $A_{projected}$)	Normalized error
1		0.176	1.45	0.057
2	3, 4, 5, 6	0.195	1.61	0.007
7	8	0.175	1.45	0.048
9		0.176	1.45	0.026

Normalized error is the root-mean-square of the difference between drag calculated using Eq. (2) and drag measurements normalized by the root-mean-square of the drag measurements.

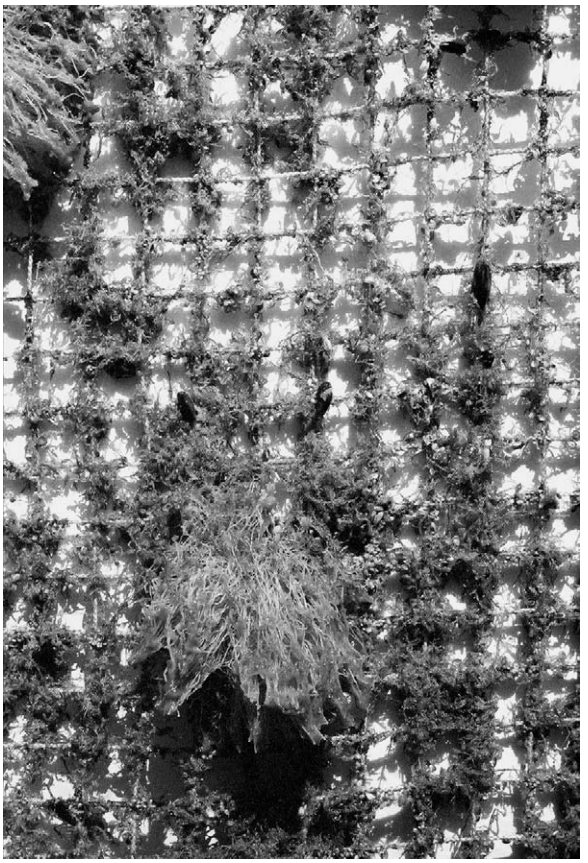

Fig. 5. Heavily fouled panel (panel 1) with *Caprella* sp. and *Tubularia* sp.

heavily fouled panels, colonial hydroids (*Tubularia* sp.) were also present (see Fig. 5). Blue mussels (*Mytilius edulus*) were distributed sparsely on all netting, but they tended to be small (approximately 1 cm in length). Larger blue mussels and rock borer clams (*Hiatella arctica*), up to 3 cm in length, were clustered along the top frame member and the very top of the netting. These probably migrated down from the grid line to which the top member was tie-wrapped. There were negligible algae due to lack of sunlight at the deployed depth. These observations were consistent with those of Greene (2004) in her study of the successional development of fouling communities on submerged cages at the OOA site. Growth mass and density, obtained by weighing in and out of water, and solidity, found photographically as described in Section 3.4. Data processing, are provided in Table 2. It should be noted that due to varying levels of toxicity as well as natural spatial variability in biological growth, nets with similar coating types accumulated differing amounts of fouling (an advantage for this study in which the dependence of drag on the extent of fouling was explored). Since the species had widely differing densities and dimensions normal to the panel, mass and solidity were taken to be independent.

Table 2
Net panel growth amounts and solidities

Net number	Mass of growth (kg)	Density (kg/m^3)	Solidity
1	5.30	1102	0.566
2	3.48	1146	0.743
3	2.70	1316	0.671
4	2.58	1196	0.813
5	5.64	1259	0.771
6	4.28	1358	0.629
7	4.96	1107	0.502
8	2.01	1255	0.572
9	3.26	1034	0.547

Maximum error in mass and density due to spring scale readings is 5%. Average error in solidity due to the imaging analysis technique, estimated as the number of ambiguous pixels divided by the number of pixels contributing to blockage, is 6%. Ambiguous pixels were those having a color common to both background and blockage.

Drag force results from tow testing in the field using the data acquisition catamaran (see Section 3.3. Field-testing of biofouled panels for procedures) typically had force-velocity dependences similar to that shown in Fig. 6. A velocity-squared relationship was fitted to each panel data set by minimizing the mean square difference (also illustrated in Fig. 6). Net-drag coefficients were then found by subtracting the frame contribution and using Eq. (2). Biofouled net drag coefficients are summarized in Table 3. Corresponding clean net values are listed as well for comparison. Outline area (1 m^2) is

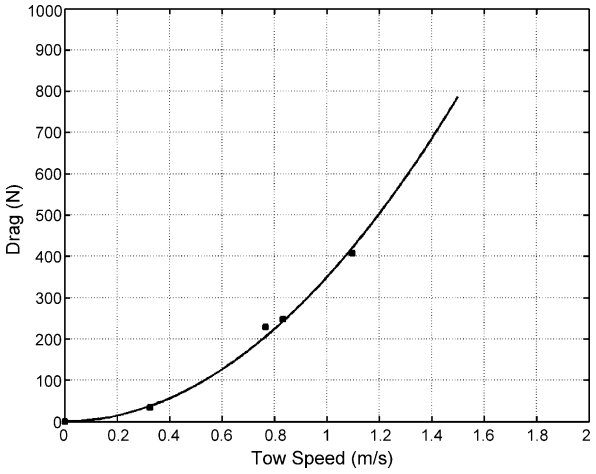

Fig. 6. Representative tow force vs. velocity data for panel 2. The dots are from field measurements, while the solid line is a best fit velocity-squared relation.

Table 3
Biofouled net-only drag coefficients compared to "clean" results

Net number	Biofouled C_D (based on $A_{outline}$)	Normalized error	"Clean" C_D (based on $A_{outline}$)	Percent increase (%)
1	0.599	0.037	0.176	240
2	0.513	0.052	0.195	163
3	0.353	0.131	0.195	81
4	0.464	0.051	0.195	138
5	0.576	0.076	0.195	195
6	0.531	0.064	0.195	172
7	0.318	0.079	0.175	82
8	0.185	0.141	0.175	6
9	0.260	0.058	0.176	48

All C_D values are from Eq. (2) using outline area (1 m^2) for A. Normalized error is the root-mean-square of the difference between drag calculated using Eq. (2) and drag measurements normalized by the root-mean-square of the drag measurements.

used for area A since in this case, thread projected area makes up only a portion of the total blockage area.

5. Discussion

For clean nets, the average drag coefficient based on projected area is comparable to that of stranded cable presented by Berteaux (1991). Specifically, the clean net average drag coefficient of 1.5 is within the range of stranded cable values of 1.4–1.6 corresponding to the experimental Reynolds number range of 0.5 (10^3)–1.7 (10^3). This suggests that for low solidities (in this case, 12.1%), the strand interaction effects are relatively small. Three of the four coating types had the same drag coefficient, but one was 11% higher. This difference may be attributed to a different surface texture but was much less than typical increases due to biofouling.

For the case of exposed nets, results presented here indicate that drag of biofouled nets may be over three times that of clean nets. The direct dependence of drag coefficient increase with solidity and growth volume may be seen in Fig. 7. From these observations, a drag coefficient of at least 0.6 (based on outline area) is recommended when designing submerged cage systems. While drag does increase generally with both solidity and volume, there is considerable scatter. This variability may be attributed in large part to the different species present. The porous blockage formed by *Caprella* sp. is expected to alter flow differently from that of deformable hydroids and that of hard shellfish. Based on the Reynolds number ranges involved and assuming fluid dynamic processes similar to those of cylinders and spheres, the filament-like *Caprella* sp. should be in the laminar regime with viscous shear playing a dominant role, while the hydroid and shellfish bodies would be subject to separated flow with the presence of form drag as well as viscous shear. Basic

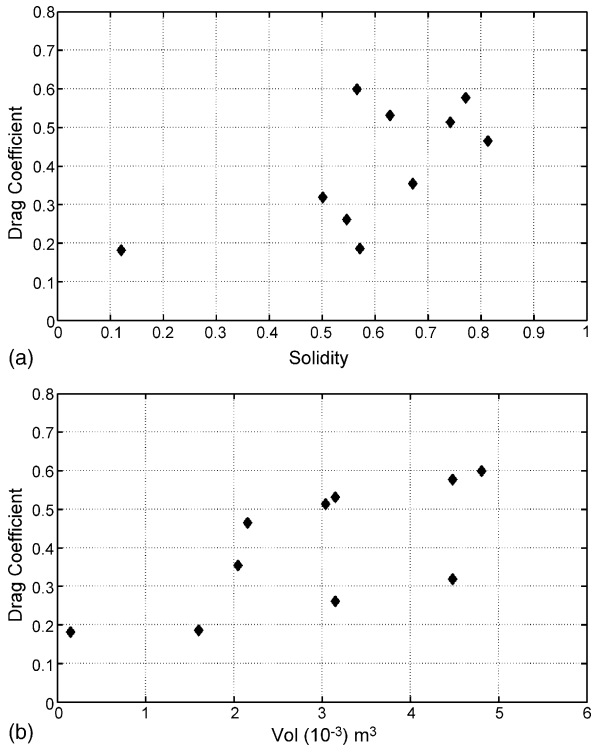

Fig. 7. Drag coefficient dependence on: (a) solidity and (b) growth volume. Drag coefficient in both cases is based on $A_{outline}$.

fluid mechanics investigations exploring this topic further would need to separate growth types, possibly making use of synthetic representations for controlled studies in tow tanks.

6. Conclusion

Biofouling increases the drag of cage nets substantially and should clearly be taken into account in design modeling for sizing cage structural components and

mooring hardware. For an anticipated biofouling mass or solidity increase, a conservative drag coefficient can be identified from the data and used to compute drag on net elements in models such as those described by Tsukrov et al. (2003) and Lader and Fredheim (2003). From a practical, operations standpoint, on the other hand, the importance of periodic net cleaning as part of a regular maintenance program should also be noted.

Acknowledgements

The authors gratefully acknowledge the contribution of Mr. G. Rice who skillfully operated the workboat during field-testing. Thanks also to Mr. J. DeCew and Mr. C. Thibeault for assisting in the field program and performing the necessary diving. In addition, we greatly appreciate the many helpful discussions with Ms. J. Greene and Prof. R. Grizzle regarding marine growth at the site. A special thank you goes to Mr. A. Walsh for expediting industrial support and providing the net panels.

This study was funded in part by the E Paint Company, the UNH Undergraduate Research Opportunities Program (UROP), and by the National Oceanographic and Atmospheric Administration (NOAA) through a grant by the UNH Cooperative Institute for New England Mariculture and Fisheries (CINEMAR).

References

Aarsnes, J.V., Rudi, H., Loland, G., 1990. Current forces on cage, net deflection. In: Engineering for Offshore Fish Farming, Thomas Telford, London, pp. 137–151.

Berteaux, H.O., 1991. Coastal and Oceanic Buoy Engineering. Woods Hole, MA, published by author.

Fredriksson, D.W., Palczynski, M.J., Swift, M.R., Irish, J.D., 2003. Fluid dynamic drag of a central spar fish cage. In: Bridger, C.J., Costa-Pierce, B.A. (Eds.), Open Ocean Aquaculture: From Research to Commercial Reality. The World Aquaculture Society, Baton Rouge, Louisiana, pp. 151–168.

Fullerton, B., Swift, M.R. Baldwin, K.C., 2002. Measurement of Drag Force Acting on Fish Cage Net Panels. Technical Memorandum, Open Ocean Aquaculture Engineering Project, University of New Hampshire, Durham, NH.

Fullerton, B., Kurgan, C., Swift, M.R., Fredriksson, D.W., 2003. Drag Force on E-Paint Treated Net Panels. Final Report submitted to E-Paint, Open Ocean Aquaculture Engineering Project, University of New Hampshire, Durham, NH.

Greene, J.K., 2004. Successional Development of Fouling Communities on Aquaculture Fish Cages in the Western Gulf of Maine, Master of Science Thesis, Zoology Department, University of New Hampshire, Durham, NH.

Kurgan, C., 2003. Fish Cage and Multiple Mooring Systems Finite Element Modeling, M.S. Thesis, Ocean Engineering, University of New Hampshire, Durham, NH.

Lader, P.F., Fredheim, A., 2003. Modeling of net structures exposed to three-dimensional waves and currents. In: Bridger, C.J., Costa-Pierce, B.A. (Eds.), Open Ocean Aquaculture: From Research to Commercial Reality. The World Aquaculture Society, Baton Rouge, Louisiana, pp. 177–189.

Lader, P.F., Fredheim, A., Lien, E., 2001. Dynamic behavior of 3D nets exposed to waves and currents. In: Proceedings of the 20th International Conference on Offshore Mechanics and Arctic Engineering, Rio de Janeiro, Brazil.

Palczynski, M.J., 2000. Fish Cage Physical Modeling, M.S. Thesis, Ocean Engineering, University of New Hampshire, Durham, NH.

Tsukrov, I., Ozbay, M., Fredriksson, D.W., Swift, M.R., Baldwin, K., Celikkol, B., 2000. Open ocean aquaculture engineering: numerical modeling. Mar. Technol. Soc. J. (Washington, DC) 34 (1), 29–40.

Tsukrov, I., Eroshkin, O., Fredriksson, D.W., Swift, M.R., Celikkol, B., 2003. Finite element modeling of net panels using a consistent net element. Ocean Eng. 30, 251–270.

Unrein, A., 2004. Design, Analysis and Construction of a Data Acquisition System for Biofouled Open Ocean Aquaculture Netting, Undergraduate Research Opportunity Program Final Report, University of New Hampshire, Durham, NH 03824.

White, F.M., 1999. Fluid Mechanics, 4th ed. McGraw-Hill, Boston, MA.